J. Phys. D: Appl. Phys. **32** (1999) 2599–2604. Printed in the UK PII: S0022-3727(99)03455-5

Phase boundaries of a uniaxial system in an applied field of arbitrary direction

Y T Millev†, H P Oepen and J Kirschner

Max-Planck-Institut für Mikrostrukturphysik, Weinberg 2, 06120 Halle, Germany

Received 14 April 1999, in final form 29 July 1999

Abstract. A procedure is put forward for the specification of a suitable phase diagram for a uniaxial system with higher-order anisotropy which undergoes a spin-reorientation transition via coherent rotation of magnetization in an applied field of arbitrary strength and direction. The approach generalizes recent studies for a field applied in one of the principal directions. The analysis is valid for bulk and thin-film systems and is relevant to all experimental techniques that involve the implementation of an external field. The representation is especially promising in the context of thickness-driven transitions in ultrathin systems. It is generally valid, beyond the uniaxial restriction, for any remagnetization process which takes place within a given plane.

1. Introduction

The motivation for this work is to understand the equilibrium behaviour of a system with higher-order uniaxial anisotropy in an external field of *arbitrary direction* and *strength*. This is pursued by finding a suitable representation (phase diagram) where the possible remagnetization processes and eventual spin-reorientation transitions are more easily described and comprehended. In particular, a parametric approach is introduced for the delineation of the phase boundaries, which lifts some of the complications arising from the assumption of a general (non-symmetric) orientation of the applied field. Usually, only the principal field configurations with the field pointing either along the axis of symmetry or perpendicularly to it are theoretically considered and practically exploited.

While the description is rather general and is valid for the coherent (Stoner–Wohlfarth) mode of remagnetization [1] in both bulk and small systems, our ultimate interest lies with the implications of the analysis to ultrathin ferromagnetic systems [2, 3]. There, considerable anisotropies are induced due to the symmetry breaking at the interfaces, whereby the anisotropy energy per spin may well be an order of magnitude larger than in the respective bulk [4]. On the other hand, the overall magnetic moment is driven into the single-domain state even by rather weak external fields.

2. The analysis

2.1. General aspects

The basis for the analysis is provided by the appropriate phenomenological anisotropy energy density g_A, which is the sum of the intrinsic uniaxial anisotropy density f_A and the unidirectional Zeeman contribution [5]:

$$g_A = f_A - \boldsymbol{H}\cdot\boldsymbol{M} = f_A - HM\cos(\theta-\phi) \qquad (1)$$

with $f_A = a\sin^2\theta + b\sin^4\theta$, where θ stands for the angle between the magnetization $\boldsymbol{M}$ and the axis of symmetry, while ϕ is the angle between the external field $\boldsymbol{H}$ and the same axis (figure 1). The anisotropy constants a and b may encompass contributions other than the purely magnetocrystalline, for instance, contributions due to magnetoelastic coupling [6]. In both bulk and thin-film systems, there exists a dipolar (shape, self-energy) anisotropy contribution to the lowest-order constant a. Orientational transitions may be triggered [7] as the balance of the various contributions to the free energy is sensitive to temperature-driven [8–10] or thickness-driven changes [3]. For the general analysis, however, it is not necessary to specify the constitution of the anisotropy constants from the very beginning.

Working at a given temperature (T) and thickness (d) and in a fixed external field of general orientation, one has to determine the equilibrium orientation of $\boldsymbol{M}$ by looking for minima of $g_A(\theta)$ via solving the equation $\mathrm{d}g_A/\mathrm{d}\theta = 0$ with $\mathrm{d}^2g_A/\mathrm{d}\theta^2 \geqslant 0$ at the points where the extremum condition is fulfilled [5]. The solutions of the minimization problem are treated as *possible orientational phases* for the uniaxial system. The problem appears standard, but leads very quickly to expressions which, for a general orientation of $\boldsymbol{H}$, could only be manipulated numerically. The important special cases of the field pointing in one of the principal directions have recently been considered in detail and on the same footing for both bulk and thin-film systems [11]. The dissatisfaction with the forbidding aspect of the

† On leave from the CPCS Laboratory, Institute of Solid State Physics, Bulgarian Academy of Sciences, 1784 Sofia, Bulgaria.

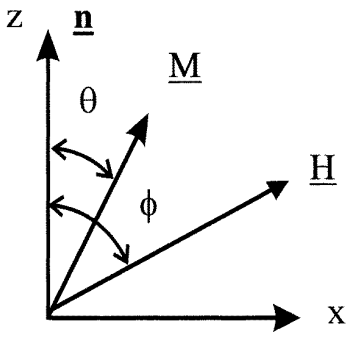

Figure 1. The relevant vectors and angular variables. The z-axis is the one of uniaxial symmetry.

solutions when higher-order anisotropies and arbitrary fields are involved is part of the motivation to look for a more insightful approach.

Most of the important work on *bulk* spin-reorientation transitions with anisotropy as high as the third non-vanishing constant was reviewed in [12] (see also [13]). It has been the rule that only the two principal field configurations were examined. Our analysis provides a parametric solution for the phase boundaries in fields of *arbitrary orientation and strength* which is valid for both bulk systems and thin ferromagnetic films. In the thin-film context further progress is achieved due to the characteristic thickness dependence of the anisotropies. The advance is disclosed as a realization of a general anisotropy-flow concept with especially simple and, hence, easily implementable linear trajectories, which are related to the relevant physical changes as described below. In the following, all of the statements and results that do not refer to, or make use of, the linearity of the trajectories are valid for both bulk and thin systems. Those statements which explicitly derive from the thickness dependence and/or the *linear* anisotropy flows relate to thin films†.

2.2. The (α, β)-space

There are three characteristic energy densities in the problem, namely, the coefficients in equation (1). We choose to scale against the Zeeman amplitude HM and remain with a dimensionless representation [11]

$$\bar{g}_A \equiv g_A/HM = \alpha \sin^2\theta + \beta \sin^4\theta - \cos(\theta - \phi) \qquad (2)$$

where $\alpha = a/HM$ and $\beta = b/HM$. We denote it as the (α, β)-representation.

It is the union of two concepts, which is especially promising for the study of reorientation transitions. The first is the stability analysis of allowed phases. It suggests the suitable phase space and serves, eventually, to analytically determine its structure, i.e. the domain of existence and stability of the different competing phases. In particular, this is the reason for studying exhaustively the (α, β)-space here, since it is especially useful for the investigation of thickness-driven transitions. The second constituent is the anisotropy-flow concept within whose framework one attempts to trace down the evolution of the system under variations of the relevant physical parameters. Even if a microscopic computational scheme‡ for the variation of the material parameters is lacking, physical restrictions and experimental conditions might help sort out a small number of *generic* scenarios [7] for the reorientation phenomenon. Thus, stability analysis sets the stage where the system is expected to evolve; in particular, crosspoints of trajectories with phase boundaries are related to spin-reorientation transitions, while the coexistence of possible phases signals hysteresis phenomena.

† This does not preclude linear anisotropy flows in bulk systems driven by, say, concentration variation or when the anisotropy flow is approximately linear over a restricted temperature range.

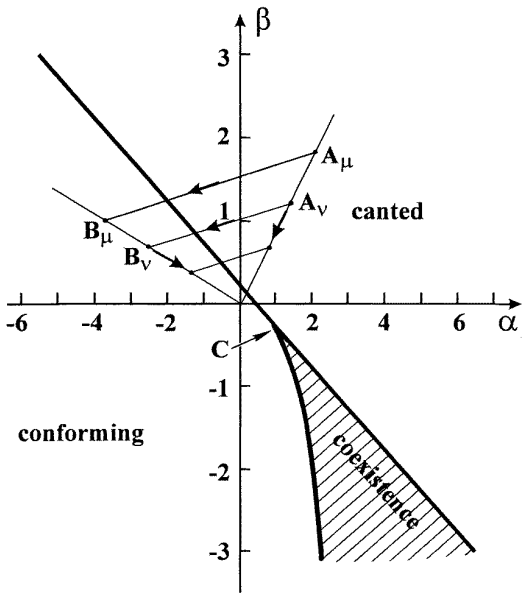

Figure 2. Linear trajectories between initial (A_μ) and final (B_μ) states for thickness-driven reorientations. In the (α, β) phase diagram, this linearity is preserved for any orientation of the applied field.

Concentrating on thickness-driven spin-reorientation transitions in ultrathin ferromagnetic films, what makes the (α, β)-representation so special is the fact that the corresponding trajectories in the (α, β)-diagram are *linear* under rather general conditions. To see this, one needs to look into the internal structure of the anisotropy constants that are characteristic of ultrathin ferromagnetic films. Quite generally, the constants are comprised of two additive contributions, a bulk-like contribution (b) and an interface of surface (s) contribution, the latter being identified by its dependence on the thickness of the sample:

$$a = K_{1b} + K_{1s} f(d) = a(d) \qquad (3)$$

$$b = K_{2b} + K_{2s} g(d) = b(d). \qquad (4)$$

The anisotropy constants K_{1b}, K_{1s}, K_{2b}, K_{2s} are material parameters which may, and normally do, depend on the temperature, but not on the thickness. Additionally, K_{1b} encompasses the demagnetization (dipolar) anisotropy energy which is $\frac{1}{2}\mu_0 M^2$ in ultrathin geometry and favours

‡ The study by Millev and Fähnle [14] provides an example where a microscopic computation of the *temperature* dependence of anisotropy within a general class of statistical–mechanical theories is possible and can be used to generate the temperature-driven anisotropy flows.

in-plane orientation of magnetization; K_{1b} also includes the magnetoelastic contributions to the anisotropy energy [6]. Whenever $f(d)$ and $g(d)$ are of the same functional form, the thickness dependence can straightforwardly be eliminated from (3) and (4) and one remains with a simple *linear* dependence between a and b:

$$b = sa + p \Rightarrow b = b(a) \tag{5}$$

where the slope s and the intercept p depend on the material parameters [7]. Equation (5) represents the linear trajectories for *thickness-driven* orientational transitions at fixed temperature. Obviously, the normalization against the Zeeman amplitude does not change the linearity and one gets $\beta = s\alpha + p \Rightarrow \beta = \beta(\alpha)$ with the same s and p as in (5)†. Obviously, the requirement for linearity, that in (3) $f(d)$ is of the same functional form as $g(d)$, is met by the widely used semi-phenomenological $1/d$-dependence of the interface anisotropies of all orders in very thin films [15–17]. Since the major effort in this paper is related to defining the phase boundaries for an *arbitrary* field, rather than implementing the said linearity, here we only summarize the important features of the linear anisotropy flows in the (α, β)-space relevant for an anisotropy energy expansion with only the first two terms kept (see also figure 2). First, the slope s of any trajectory is independent of the field and equals the ratio of the first two *surface* anisotropy constants K_{2s}/K_{1s}. Hence, trajectories corresponding to different field magnitudes are parallel to each other. Second, for a given system the intercept of any trajectory with the ordinate is inversely proportional to the field. For $H \to \infty$, the intercept goes to zero. Both statements are true for *any* orientation ϕ of the field; this extends previous findings on these aspects of the trajectories [11]. For $H \to 0$, the intercept and the trajectory itself go to infinity in accordance with the fact that, by the chosen normalization, the zero-field case cannot be 'observed' in this representation. Like the slope mentioned above, the sign of the intercept is independent of the field. Hence, for a given system, the sign of intercept and the slope of trajectory are invariants of this representation and do not depend on the field strength for any field orientation. In summary, the isolines of constant thickness are represented by the family of rays going into the origin with increasing field, while the isolines of constant field are given by the family of parallel segments $\{A_\mu B_\mu\}$ connecting initial and final states of the system, as represented by the respective points in the diagram (figure 2). These are the eventual thickness-driven trajectories. In figure 2 we have chosen the principal configuration of an external field applied perpendicularly to the easy axis in order to illustrate the (α, β)-space and the linear trajectories. What is specific here are the thick phase boundaries, while for a given system (a given set of material parameters) the trajectories are invariant. For the perpendicular configuration shown, $\beta = -\frac{8}{27}\alpha^3$ (the curvilinear boundary) and $\beta = \frac{1}{4} - \alpha/2$ (the linear boundary). The problem addressed in the paper is to determine the phase boundaries for *any* orientation of the applied field.

With this knowledge, we proceed to determine the *structure* of the chosen phase space ((α, β)-representation) by delineating the boundaries of stability of the possible solutions for *any* orientation of the applied field. We remind the reader that the possible stable solutions are also referred to as 'phases'.

2.3. The field-aligned (conforming) solutions

As might be expected, these are the easiest to describe. Still, when the field is of an arbitrary orientation, there are some aspects which have not been sufficiently elucidated. We impose the condition of a conforming magnetization $\theta = \phi$. The respective solutions have the same formal appearance as those characteristic of the case without an applied field [7], namely, (i) $\theta = \phi = 0$, the coaxial conforming solution‡, which is stable for $\alpha \geqslant -\frac{1}{2}$; (ii) $\theta = \phi = \pi/2$, the perpendicular conforming solution which is stable for $\beta \leqslant -\alpha/2$; (iii) $\theta = \phi \neq 0, \pi/2$, a generalized canted solution which deserves a more careful description. If the so-called anisotropy fields [18] are introduced as $H_{A1} \equiv 2|a|/M$ and $H_{A2} \equiv |2a + 4b|/M$, the conditions for the principal configurations (i) and (ii) are often expressed as $|\boldsymbol{H}| > H_{A1}$ and $|\boldsymbol{H}| > H_{A2}$, respectively. In case (iii), the magnetization must point along $\boldsymbol{H}$ in a direction different from any of the two principal orientations. For a fixed ϕ, the solution is specified by

$$\sin^2\theta = \sin^2\phi = -\alpha/2\beta = -a/2b \tag{6}$$

with the additional restriction of $-2 \leqslant \alpha/\beta \leqslant 0$, stemming from the obvious condition $0 \leqslant \sin^2(x) \leqslant +1$. It transpires that, for a strictly field-aligned phase in a field of general orientation to exist, it is necessary that $\alpha\beta < 0$, i.e. the intrinsic anisotropy constants a and b must be of different signs. Thus, in both the (a, b)- and (α, β)-representations which have been introduced as especially informative for the analysis of no-field [7] and in-field [11] reorientation transitions in thin films and bulk systems, the generalized conforming solution is tolerated within (portions of) the second or fourth quadrants. The precise delineation of its existence and stability is given by the conditions:

$$\beta > 0, \alpha < 0: \quad \beta > -\alpha/2 \tag{7}$$

† To make the terminology absolutely transparent, we refer to the case of a classical motion of a system with two degrees of freedom, say, x and y. The *laws* of motion are found by eventually solving Newton's equations of motion and have the form $x = x(t)$, $y = y(t)$, while the trajectories in the two-dimensional space are eventually obtained by the elimination of the evolution parameter (time), so that $y = y(x)$ or $x = x(y)$ is the equation of the trajectory. The solution of the Keplerian problem is a good example to think about (with the polar coordinates ρ and ϕ instead of x and y). Other enlightening analogies are provided by phase portraits of dynamical systems where coordinate and conjugate momentum are directly related after eliminating time; a vast group of examples is provided by renormalization-group flows as driven by a scaling transformation in the parameter space of the Hamiltonian of the problem.

‡ The terminology we use is simply related to the important features of the corresponding solutions (cf figure 1). Thus, 'coaxial' means that the direction of $\boldsymbol{M}$ coincides with that of the crystallographic axis $\boldsymbol{n}$ of rotational (uniaxial) symmetry ($\theta = 0$), 'perpendicular' refers to $\boldsymbol{M}$ being perpendicular to $\boldsymbol{n}$ ($\theta = \pi/2$), while 'conforming' and 'non-conforming' refer to the mutual orientation of the pair of vectors $\boldsymbol{M}$ and $\boldsymbol{H}$. $\boldsymbol{M}$ conforms with $\boldsymbol{H}$ when $\phi = \theta$ and is non-conforming otherwise. Finally, the term 'canted' is used for a situation when $\boldsymbol{M}$ is canted with respect to $\boldsymbol{n}$, i.e. the angle θ is neither zero or ninety degrees. Since a canted solution in a system with two anisotropy constants exists even without an external field, we use the term 'generalized canted solution' for a canted solution in an applied field.

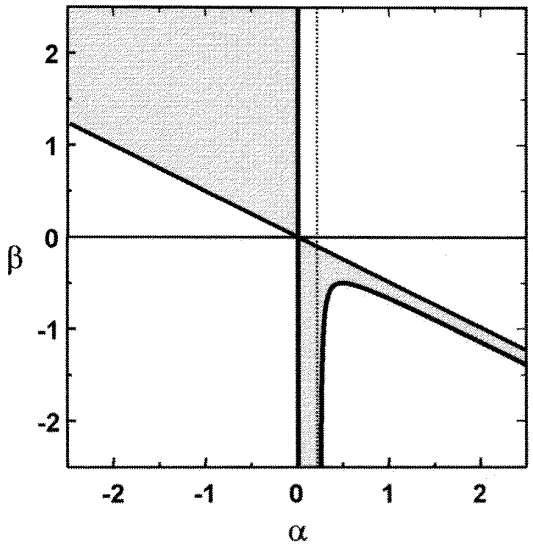

Figure 3. Regions in the (α, β)-diagram where a field-aligned (conforming) solution is possible are given shaded. The thick boundaries are defined in (7)–(9).

$$\beta < 0, 0 < \alpha < 1/4: \quad \beta < -\alpha/2 \tag{8}$$

$$\beta < 0, \alpha > 1/4: \quad -\alpha/2 > \beta > 2\alpha^2/(1-4\alpha). \tag{9}$$

In figure 3, the shaded regions correspond to the existence and stability of a generalized conforming phase (i.e. saturation in a field pointing in a non-principal direction). It follows immediately that there are large portions of the phase diagram where no saturation is possible, i.e. the normalized field-resolved magnetization can never be equal to unity. Ideally, even a very strong field, which corresponds to the vicinity of the origin in this representation, will not be able to force the magnetization vector into alignment if the material parameters are such that the system belongs to either of the larger unshaded symmetric wedges coming together at the origin (figure 3)†. It is the physical counteraction of torques caused by the external magnetic field and the effective anisotropy fields which underlies the outcome of the analysis. One should view figure 3 as the pictorial expression of this competition. While the lack of saturation and the related approach to saturation belong to the established operational notions of magnetism [19], a diagram such as that given in figure 3 appears new and has the advantage of shedding light on the problem of saturation in the present context. Note, that for a field of prescribed orientation the conforming solution is possible on that portion of the unique line $\beta = -\alpha/2\sin^2\phi$ which falls within the shaded region in figure 3. Thus, full saturation along the field direction is only realized if the varying parameter (thickness, temperature, etc) drives the system across this line by modifying the anisotropies in the system. Note, that this diagram is very general and is not restricted to thickness-driven transitions. In the latter case, the trajectories under variation would be lines which facilitates the analysis.

† Note that in an experimental setting it might be difficult to distinguish a complete saturation from a 'near-saturation'; the latter will appear to take place even in the 'forbidden' (unshaded) regions of figure 3 when the field is strong enough.

Furthermore, the shaded region in the second quadrant of figure 3 corresponds precisely to the region in the anisotropy space (a, b) of the system, where a 'true' canted phase is possible even in the absence of an applied field. Its centrosymmetric wedge in the fourth quadrant (the one obtained by changing the signs of both anisotropy constants simultaneously) corresponds to the case of coexistence of the perpendicular and coaxial phases in zero field. In view of the competition between these two zero-field phases, one needs fields of sufficient magnitude to be able to saturate the system. In terms of the diagram in figure 3, this means that the system has to be forced into the shaded portion by increasing the field (remember that stronger fields here correspond to locations closer to the origin). Thus, the asymmetry of the zero-field anisotropy space reappears in the (α, β) with-field representation in a remarkable way.

The diagram of figure 3 also gives a clue to the understanding of the complicated asteroids in $\boldsymbol{H}$-space, which come about in the presence of higher-order anisotropies [20]; in particular, it has been noted [20] that the asteroids which differ by the interchange of signs of the two constants have an identical appearance, while the reversal processes are, of course, different [21–24]. With the help of the diagram in figure 3, one can identify the relevant branches for each set of signs of α and β, thereby removing an undesired and unphysical ambiguity already at the general level of the analysis.

2.4. The phase boundaries for the non-conforming solutions

These are determined as the critical lines where some of the physically allowed solutions grow unstable. Hence, keeping the orientation ϕ as a parameter, the defining equations for these lines are

$$\mathrm{d}\bar{g}_A/\mathrm{d}\theta = \mathrm{d}^2\bar{g}_A/\mathrm{d}\theta^2 = 0. \tag{10}$$

We arrange the two equations as a simple linear system for the determination of $\alpha = a/HM$ and $\beta = b/HM$ which is then solved. Explicitly, and this is our parametric solution,

$$\alpha_c(\theta;\phi) = \frac{\sin^2\theta}{\sin^3 2\theta}[\sin 2\theta\cos(\theta-\phi) + 2(4\sin^2\theta - 3)\sin(\theta-\phi)] \tag{11}$$

$$\beta_c(\theta;\phi) = \frac{1}{2\sin^3 2\theta}[\cos 2\theta\sin(\theta-\phi) - \sin(\theta+\phi)]. \tag{12}$$

In this solution, the critical curve $\beta_c(\alpha_c)$ is obtained by fixing the orientation ϕ of the external field and letting the sweeping parameter θ vary within the range $(-\pi, +\pi)$. Thus, one has at once a versatile tool for extracting the most important features of the behaviour of a uniaxial system in an external field of arbitrary orientation.

The solution just given encompasses as particular cases the two principal field orientations. For the coaxial field configuration, set $\phi = 0$ in (7)–(8), eliminate θ to get

$$\alpha = \alpha(\beta) = -2\beta + \tfrac{3}{2}\beta^{1/3}. \tag{13}$$

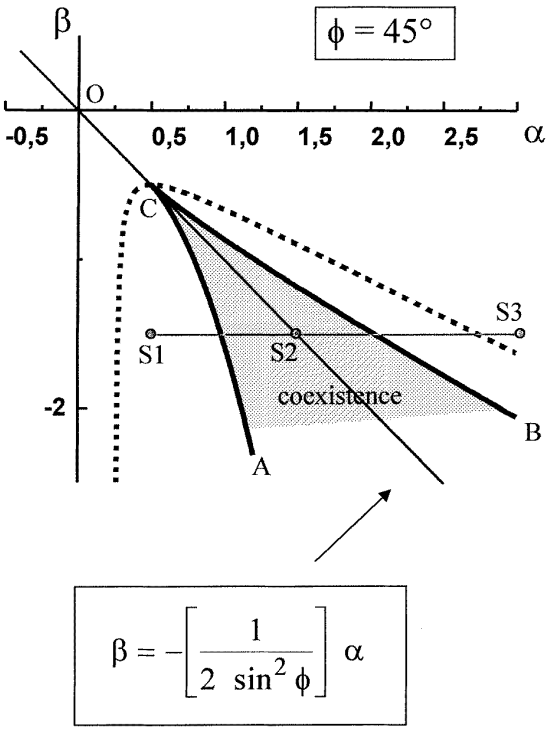

Figure 4. Phase boundaries for a field making an angle $\phi = \pi/4$ with the crystallographic axis. The shaded region is where two non-conforming minima exist. The line is the particular $\phi = \pi/4$ case of the equation for the canted conforming solution, $\beta = -\alpha/2\sin^2\phi$. Only the portion of the line above the point C corresponds to a canted conforming minimum ($\boldsymbol{M}$ is aligned with $\boldsymbol{H}$, while both are askew to the crystallographic axis). The point C is a tricritical point. There, the canted conforming solution ceases to be a minimum. The precise location of C is specified for any given ϕ by reading its coordinates off from the corresponding parametric solution for that value of ϕ.

For the *perpendicular* configuration, set $\phi = \pi/2$ and eliminate θ to get

$$\alpha = \alpha(\beta) = -\tfrac{3}{2}\beta^{1/3} \qquad (\beta(\alpha) = -\tfrac{8}{27}\alpha^3). \tag{14}$$

These were the explicit critical lines found in [11]. One recognizes the availability of a substantially more general solution for the critical boundary.

In figure 4, the critical boundary for the particular case $\phi = \pi/4$ is given. There is only one minimum of the free energy along any path outside the wedge ACB. The portion within the curvilinear wedge tipping at C is that part of the (α, β)-space where two non-conforming minima $0 < \theta < \pi/2$ coexist (magnetization non-aligned with field). This can be seen from continuity arguments based on the respective (α, β)-diagrams for the principal field configurations [11], or by looking directly at the free energy landscape along a representative cut across the wedge of coexistence. This is done in figure 5, where we took the cut $S_1S_2S_3$ as defined in figure 4 for $\phi = \pi/4$ with $S_1(0.5, -1.5)$, $S_2(1.5, -1.5)$, and $S_3(3, -1.5)$. Outside the domain of coexistence ACB, one finds a unique minimum corresponding to a unique non-conforming phase ($\theta \neq 0; \pi/2$). Within, there are two minima corresponding to orientations of magnetization that are canted with respect

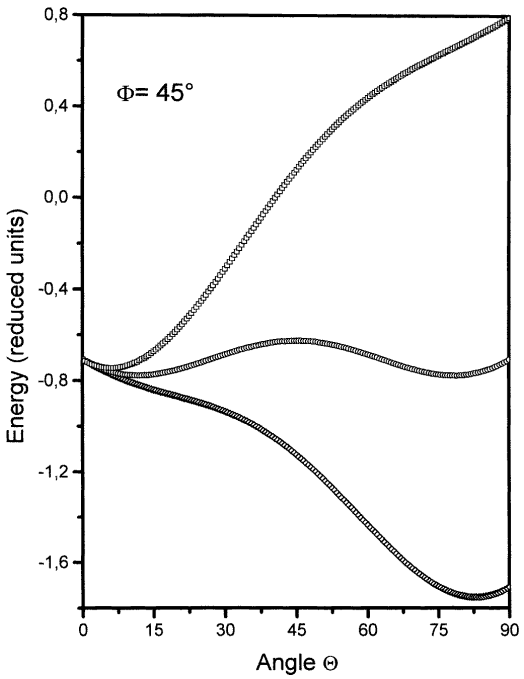

Figure 5. The anisotropy energy profiles for an external field at an angle $\phi = 45^\circ$ with the crystallographic axis. The curves correspond, from the top, to the points S_1, S_2, and S_3 in figure 4. Within the region of coexistence (shaded region in figure 4), there are two competing stable states.

to the principal directions and are separated by a certain barrier. The height of the barrier, which might be of interest for the study of relaxation phenomena, can be easily determined from such plots with the relevant values for the pair (α, β). The middle curve is taken precisely at the point S_2 where both competitors are equally stable (their minima are equally deep). The maximum separating them is precisely at $\theta = \phi = 45^\circ$. Note that on moving along the S_2C in figure 4 towards C this maximum gets lower and the two minima get closer until at C they merge together; beyond that point, the ray CO is a locus of stable generalized conforming states for this orientation of the applied field ($\phi = 45^\circ$). The point C in this phase diagram is a tricritical point [5]. Geometrically, C lies on the unique common tangent to the two curvilinear boundaries which is precisely the line $\beta = -\alpha/2\sin^2\phi$. Its origin can be traced back to the respective tricritical points described in detail for the two principal field configurations [11]. Precisely at the tricritical point C whose coordinates for $\phi = \pi/4$ are given by $\alpha = -\beta = \frac{1}{2}$, the free energy minimum is very flat, as can be easily checked by plotting the energy landscape. With the help of the parametric approach as outlined above, one can easily see that small deviations of the field orientation out of the principal directions causes small continuous deformations of the region of coexistence. The same is true for the shift of the tricritical point. Since our solution allows one to work with *any* $\phi \in [0, \pi]$, one can also actually describe the trajectory of this very special point as driven by the change of orientation of the applied field†.

† For $\phi = 0$, the tricritical point is at $(\alpha = -1/2, \beta = -1/8)$, while for $\phi = \pi/2$ it is at $(\alpha = 3/4, \beta = -1/8)$. For an arbitrary field orientation (arbitrary ϕ), the coordinates can be read off from the parametric plot with the corresponding value of ϕ.

The full analysis requires that the regions and conditions of stability of both conforming and non-conforming solutions be examined together. Hence, a 'superposition' of figures 3 and 4 must be considered. There arise no interpretational difficulties in the process. Fixing $\phi = \pi/4$ as for figure 4, one singles out the line $\beta = k\alpha$ with $k = -1/2\sin^2\phi = -1$. It hits the tricritical point. Only on the ray CO can there exist a full alignment. On the other hand, a thickness-driven process is described by a linear trajectory in the (α, β)-space, as explained above (see figure 2). Hence, the generalized conforming phase (complete alignment) has to be considered at a unique point in the diagram, if at all, and this is the eventual crossing point of the linear trajectory with the ray CO ($\beta = -\alpha$). From our diagrams of stability, it is obvious that such a situation can only arise, if at all, in the second or fourth quadrants. Keeping ϕ fixed and working in successively weaker $|\boldsymbol{H}|$, one may deduce information about the relevant quadrant, since the eventual full-alignment crosspoint will necessarily disappear for $H \to 0$ in the fourth quadrant, but will definitely persist the whole way down to $H = 0$ in the second quadrant (whereby α and β go to infinity by definition) as the explicit equations we derived for the boundaries in figure 2 indicate. From an experimental point of view, however, it is much more promising to use the information given in this paper to study the response to a small perturbing field in susceptibility, ferromagnetic-resonance, or Brillouin-light-scattering experiments. Such methods should allow one to sense the peculiarities and singularities related to crosspoints between trajectories and phase boundaries by choosing properly the external (bias) field and exploiting specific information about the material parameters of the given system which is explored.

3. Summary

Using an appropriate parametric approach combined with a suitable two-dimensional representation, we describe the region of coexistence of competing minima for a uniaxial system in a field of arbitrary orientation and magnitude. Because of the linearity of the thickness-driven evolution in the chosen representation, simple topological considerations are possible, which provide the necessary qualitative and quantitative insights in a rather straightforward way. One of the important reasons to investigate the uniaxial case in sufficient detail is that the method applies to any process in an external field, regardless of whether the anisotropy symmetry is uniaxial or not, given that the magnetization remains within the same plane all along. In particular, reorientations within the plane of an ultrathin film in an external field can be described successfully [25, 26]. The case of the so-called *fourfold* in-plane anisotropy is also a particular case of our study with $\alpha/\beta = a/b = -1$. The effects of the additional characteristic step-induced uniaxial surface anisotropies [27, 28], whether large or small in comparison with the fourfold one, are readily illuminated for any direction of the in-plane field. The phase diagrams which can now be constructed for a field of arbitrary orientation provide a basis for systematic studies of the response of ultrathin systems with orientational transitions to small perturbing fields.

References

[1] Stoner E C and Wohlfarth E P 1948 *Phil. Trans. R. Soc.* A **240** 599
[2] Heinrich B and Cochran J F 1993 *Adv. Phys.* **42** 523
[3] Bland J A C and Heinrich B (eds) 1994 *Ultrathin Magnetic Structures I* (Berlin: Springer)
[4] Farle M 1998 *Rep. Prog. Phys.* **61** 755
[5] Landau L D and Lifshitz E M 1960 *Electrodynamics of Continuous Media* (Oxford: Pergamon) ch 5
[6] du Tremolet de Lacheisserie E 1993 *Magnetostriction: Theory and Applications of Magnetoelasticity* (Boca Raton, FL: CRC Press)
[7] Millev Y and Kirschner J 1996 *Phys. Rev.* B **54** 4137
[8] Millev Y and Fähnle M 1995 *Phys. Rev.* B **52** 4336
[9] Jensen P J 1997 *Acta Phys. Pol.* A **92** 427
[10] Ecker A, Fröbrich P, Jensen P J and Kuntz P J 1999 *J. Phys.: Condens. Matter* **11** 1557
[11] Millev Y T, Oepen H P and Kirschner J 1998 *Phys. Rev.* B **57** 5837
Millev Y T, Oepen H P and Kirschner J 1988 *Phys. Rev.* B **57** 5848
[12] Asti G 1990 *Ferromagnetic Materials* vol 3, ed K H J Buschow and E Wohlfarth (Amsterdam: Elsevier) pp 398–464
[13] Nieber S and Kronmüller H 1991 *Phys. Status Solidi* b **165** 503
[14] Millev Y and Fähnle M 1995 *J. Phys.: Condens. Matter* **7** 6909
[15] Néel L 1954 *J. Phys. Radium (Paris)* **15** 225
[16] Gradmann U 1993 *Handbook of Magnetic Materials* vol 7, ed K H J Buschow (Amsterdam: North-Holland) ch 1
[17] Millev Y T, Skomski R and Kirschner J 1998 *Phys. Rev.* B **58** 6305
[18] Zijlstra H 1967 *Experimental Methods in Magnetism* (Amsterdam: North-Holland) ch 5
[19] For a very recent progress and discussion, cf J F Herbst and F E Pinkerton 1998 *Phys. Rev.* B **57** 10 733
[20] Millev Y T, Cullen J R and Oepen H P 1998 *J. Appl. Phys.* **83** 6500
[21] Mitsek A I, Kolmakova N P and Sirota D I 1974 *Fiz. Met. Metall.* **38** 35
[22] Chang C-R and Fredkin D R 1988 *J. Appl. Phys.* **63** 3435
[23] De Jesus J C O and Kleemann W 1997 *J. Magn. Magn. Mater.* **169** 159
[24] Thiaville A 1998 *J. Magn. Magn. Mater.* **182** 5
[25] Fruchart O, Nozieres J-P and Givord D 1997 *J. Magn. Magn. Mater.* **165** 508
[26] Brockmann M, Miethaner S, Onderka R, Köhler M, Himmelhuber F, Regensburger H, Bensch F, Schweinböck T and Bayreuther G 1997 *J. Appl. Phys.* **81** 5047
[27] Berger A, Linke U and Oepen H P 1992 *Phys. Rev. Lett.* **68** 839
[28] Wulfhekel W, Knappmann S and Oepen H P 1996 *J. Appl. Phys.* **79** 988